

Ethylene Oxide Functionalization Enhances Ionic Conductivity of a MOF

Sorout Shalini^a and Adam J. Matzger^{*a,b}

^a Department of Chemistry, University of Michigan, 930 North University Avenue, Ann Arbor, MI 48109, USA

^b Department of Macromolecular Science and Engineering, University of Michigan, Ann Arbor, MI 48019, USA

*To whom correspondence should be addressed. Email address: matzger@umich.edu

Table of contents.

SI 1. Experimental Methods

SI 2. NMR

SI 3. Simulated and experimental PXRD patterns of MOFs

SI 4. N₂ sorption isotherms for UiO-68-EO and UiO-68-2EO

SI 5. Cyclic DSC of UiO-68-2EO/LiTFSI composites

SI 6. PXRD of MOF-salt composites

SI 7. AC impedance spectroscopy

SI 8. References

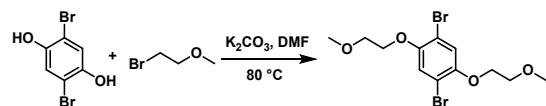
SI 1. Experimental Methods

2,5-Dibromohydroquinone (97%), magnesium sulfate (99.5%), and 1-bromo-2-methoxyethane were purchased from Sigma Aldrich. Anhydrous K_2CO_3 (99.3%) and benzoic acid (99.9%) were purchased from Fisher Scientific. (4-(methoxycarbonyl)phenyl)boronic acid (>97%) and 4-methoxycarbonylphenylboronic acid pinacol ester (>97%) were purchased from Boron Molecular. Palladium-tetrakis(triphenylphosphine) (99%) and $ZrCl_4$ (99.95%) were purchased from STREM Chemicals. 1-Bromo-2-(2-methoxyethoxy)ethane was purchased from Tokyo Chemical Industry. HCl (36.5-38.0% w/w), NH_4OH (28%), DMF (99.8%), methanol (99.8%), and ethyl acetate (99.5%) were purchased from Fisher Scientific. Ethanol was purchased from Decon Labs. Anhydrous DMF (99.5%) was purchased from Acros Organics.

Linker synthesis:

Linker for UiO-68-EO

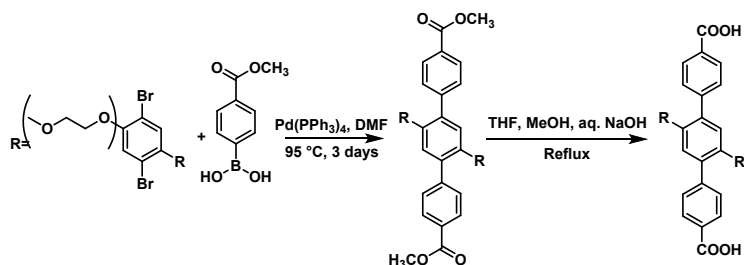
Step 1. A representative synthesis of 1,4-dibromo-2,5-bis(2-methoxyethoxy)benzene (adapted for 1,4-dibromo-2,5-bis(2-methoxyethoxy)benzene from Uribe-Romo et al¹): 2,5-Dibromohydroquinone (2 g, 7 mmol) and K_2CO_3 (6.1 g, 44 mmol) were loaded in a Schlenk flask which was evacuated and backfilled with N_2 three times. Anhydrous dimethylformamide (DMF, 32 mL) and 1-bromo-2-methoxyethane (1.46 mL, 15.5 mmol) were added to the flask dropwise under N_2 while stirring with a magnetic stir bar. The contents were stirred at RT for 4 hours and then heated at 80 °C for 42 hours. The reaction mixture was allowed to cool to RT and quenched with 1 M aq. HCl (22 mL). The flask was then kept at 0 °C for 12 hours. The product 1,4-dibromo-2,5-bis(2-methoxyethoxy)benzene was collected via filtration and recrystallized from methanol at -78 °C. NMR shown in figure S1.



Step 2. A representative synthesis of dimethyl 2',5'-bis(2-methoxyethoxy)-[1,1':4',1''-terphenyl]-4,4''-dicarboxylate: In a 150 mL glass pressure vessel, DMF (55 mL) was sparged with N_2 for 30 minutes. 1,4-Dibromo-2,5-bis(2-methoxyethoxy)benzene (2.7 g, 7.0 mmol), (4-(methoxycarbonyl)phenyl)boronic acid (3.16 g, 17.5 mmol), palladium-tetrakis(triphenylphosphine) (406 mg, 0.351 mmol), and K_2CO_3 (4.8 g, 34 mmol) were added to the DMF. The pressure vessel was flushed with N_2 before being sealed and heated at 90 °C for 3 days with stirring. The reaction was quenched with ice cold water. The product was collected via filtration and air dried. It was then dissolved in ethyl acetate and washed with water followed by ~ 2M HCl (25 mL) and brine (25 mL). The organic layer was stirred with activated carbon and anhydrous magnesium sulfate for 1 hour and then filtered. The filtrate was concentrated under reduced pressure. The obtained residue was refluxed in methanol (75 mL) overnight and passed

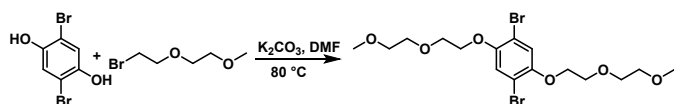
through celite plug while hot. Methanol was evaporated under reduced pressure yielding dimethyl 2',5'-bis(2-methoxyethoxy)-[1,1':4',1''-terphenyl]-4,4''-dicarboxylate).

Step 3. A representative synthesis of 2',5'-bis(2-methoxyethoxy)-[1,1':4',1''-terphenyl]-4,4''-dicarboxylic acid: Dimethyl 2',5'-bis(2-methoxyethoxy)-[1,1':4',1''-terphenyl]-4,4''-dicarboxylate (3 g, 6 mmol) was dissolved in a THF/MeOH solution (1:1, 100 mL). To this solution, aq. NaOH (5.5 g in 45 mL H₂O) was added dropwise with stirring and the solution was heated to reflux for 24 h. The reaction mixture was allowed to cool to RT and the THF/MeOH evaporated under reduced pressure. The pH was adjusted to ~2 using dil. HCl. and the product was collected via filtration, rinsed with water and air dried. To remove residual palladium from step 2, the crude product was dissolved with 28% NH₄OH aq. solution (30 mL) in a 45 mL solvothermal bomb (Parr instrument company model 4744 general purpose acid digestion vessel) and held at 170 °C overnight in an oven. After cooling to ambient, the pH was adjusted to ~2 using dil. HCl and the product collected by vacuum filtration, rinsed with water and dried under vacuum. NMR shown in figure S2.



Linker for UiO-68-2EO

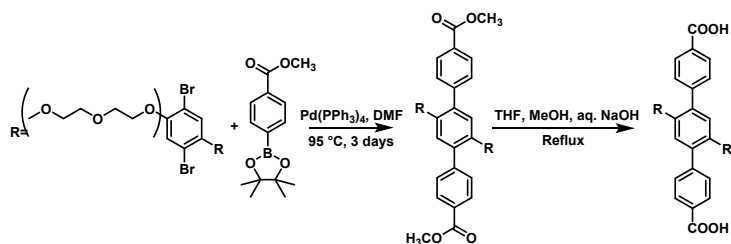
Step 1. Synthesis of 1,4-dibromo-2,5-bis(2-(2-methoxyethoxy)ethoxy)benzene (adapted for 1,4-dibromo-2,5-bis(2-(2-methoxyethoxy)ethoxy)benzene from Uribe-Romo et al¹): 2,5-Dibromohydroquinone (503 mg, 1.87 mmol) and K₂CO₃ (1.53 g, 11.1 mmol) were loaded in a Schlenk flask which was evacuated and backfilled with N₂ three times. Anhydrous DMF (8 mL) and 1-bromo-2-(2-methoxyethoxy)ethane (0.520 mL, 3.87 mmol) were mixed together and added to the flask dropwise under N₂ while stirring with a magnetic stir bar. The contents were stirred at RT for 4 hours and then heated at 80 °C for 42 hours. The reaction mixture was allowed to cool to RT and quenched with 1 M aq. HCl (5.5 mL). The flask was then kept at 0 °C for 12 hours. The product (1,4-dibromo-2,5-bis(2-(2-methoxyethoxy)ethoxy)benzene) was collected via filtration and recrystallized from methanol at -78 °C. NMR shown in figure S3.



Step 2. Synthesis of dimethyl-2',5'-bis(2-(2-methoxyethoxy)ethoxy)-[1,1':4',1''-terphenyl]-4,4''-dicarboxylate: In a 150 mL glass pressure vessel, DMF (45 mL) was sparged with N₂ for 30 minutes. 1,4-Dibromo-2,5-bis(2-(2-methoxyethoxy)ethoxy)benzene (2.36 g, 4.99 mmol), 4-

methoxycarbonylphenylboronic acid pinacol ester (3.27 g, 12.5 mmol), palladium-tetrakis(triphenylphosphine) (289 mg, 0.250 mmol), and K_2CO_3 (3.45 g, 24.9 mmol) were added to DMF. The pressure vessel was flushed with N_2 before being sealed and heated at 90 °C for 3 days with stirring. The reaction was quenched with ice cold water. The product was collected via filtration and air dried. It was then dissolved in ethyl acetate and washed with water followed by ~ 2M HCl (20 mL) and brine (20 mL). The organic layer was stirred with activated carbon and anhydrous magnesium sulfate for an hour and then filtered. The filtrate was concentrated under reduced pressure. The obtained residue was refluxed in methanol (50 mL) overnight and passed through celite plug while hot. Methanol was evaporated under reduced pressure yielding dimethyl 2',5'-bis(2-(2-methoxyethoxy)ethoxy)-[1,1':4',1''-terphenyl]-4,4''-dicarboxylate.

Step 3. Synthesis of 2',5'-bis(2-(2-methoxyethoxy)ethoxy)-[1,1':4',1''-terphenyl]-4,4''-dicarboxylic acid: Dimethyl-2',5'-bis(2-(2-methoxyethoxy)ethoxy)-[1,1':4',1''-terphenyl]-4,4''-dicarboxylate (2.08 g, 3.57 mmol) was dissolved in a THF/MeOH solution (1:1, 150 mL). To this solution, aq. NaOH (3.84 g in 30 mL H_2O) was added dropwise with stirring and the solution was heated to reflux for 24 h. The reaction mixture was allowed to cool to RT and the THF/MeOH evaporated under reduced pressure. The pH was adjusted to ~2 using dil. HCl and the product was collected via filtration, rinsed with water and air dried. To remove residual palladium from step 2, the crude product was dissolved with 28% NH_4OH aq. solution (45 mL). It was divided in two parts and transferred to 2, 45 mL solvothermal bombs (Parr instrument company model 4744 general purpose acid digestion vessel) and held at 170 °C overnight in an oven. After cooling to ambient, the pH was adjusted to ~2 using dil. HCl and the product collected by vacuum filtration, rinsed with water and dried under vacuum. NMR shown in figure S4.



MOF synthesis:

PCN-56: PCN-56 was synthesized using method previously reported.²

UiO-68-EO: $ZrCl_4$ (29.7 mg, 0.127 mmol) and benzoic acid (78.5 mg, 0.643 mmol) were dissolved in DMF (15 mL) in a 20 mL vial. The linker (69.7 mg, 0.149 mmol) and H_2O (20 μ L) were added to the vial, which was then sealed and heated at 70 °C for 3 days. The reaction mixture was allowed to cool to RT, centrifuged, and the product collected by decanting the mother liquor and washing with DMF (3×15 mL). The resulting solid was then soaked in ethanol (15 mL) for one day, during which the ethanol was decanted and replenished thrice. The solid was then dried under vacuum. The typical yield of the reaction, determined from the weight of the solvent-free material, is 20 to 30% based on the linker.

UiO-68-2EO: ZrCl_4 (20.6 mg, 0.0883 mmol) and benzoic acid (53.3 mg, 0.436 mmol) were dissolved in DMF (10 mL) in a 20 mL vial. The linker (55.9 mg, 0.101 mmol) and H_2O (18 μL) were added to the vial, which was then sealed and heated at 70 °C for 5 days. The reaction mixture was allowed to cool to RT, centrifuged, and the product collected by decanting the mother liquor and washing with DMF (3×15 mL). The resulting solid was then soaked in ethanol (15 mL) for one day, during which the ethanol was decanted and replenished thrice. The solid was then dried under vacuum. The typical yield of the reaction, determined from the weight of the solvent-free material, is 30 to 35% based on the linker.

A general procedure for salt loading:

1. The MOFs were activated by exposure to a dynamic vacuum ($\sim 10^{-2}$ Torr) at 90 °C for 18 hours.
2. Under an inert atmosphere (N_2), the MOF (ca. 30.0 mg) and salt (ratios provided in main text) were ground together using a mortar and pestle.
3. The ground MOF-salt mixture was then sealed in a glass vial (4 mL) under an inert atmosphere (N_2).
4. The loaded vial was then heated at 235 °C for 30 minutes and the obtained composite allowed to free-cool to ambient temperature.
5. As the MOF and salt were both dry/preactivated there was no further need for activation/drying of the obtained composites.
6. PXRD and DSC were used to verify complete salt loading.

PXRD data were collected on a PANalytical Empyrean diffractometer in Bragg–Brentano geometry using $\text{Cu-K}\alpha$ radiation (1.54187 Å), operating at 45 kV and 40 mA. The incident beam was equipped with a Bragg-BrentanoHD X-ray optic using fixed slits/soller slits. The detector was a silicon-based linear position sensitive X'Celerator Scientific operating in 1-D scanning mode. The samples were ground using a mortar and pestle to minimize preferred orientation and the data were collected from 5° to 50° 2θ with a step size of 0.008°.

Nitrogen sorption isotherms were measured on a NOVA e-Series 4200 surface area analyzer (Quantachrome Instruments). N_2 (99.999%) was purchased from Cryogenic Gases and used as received. Sorption isotherms were analyzed by NOVAwin software. For each N_2 measurement, a glass sample cell was charged with ~ 40 mg sample and analyzed at 77 K.

Cyclic DSC experiments were carried out on TA Instrument Q20 differential scanning calorimeter. Precisely weighed samples were placed in Tzero™ hermetic aluminum pans and heated from 30 to 250 °C at a heating rate of 10 °C/min under nitrogen atmosphere, held at 250 °C for 5 minutes, and cooled back to 30 °C at 10 °C/min. For the subsequent cycles the hold time varied from an hour to 8 hours until the melt endotherm of the salt disappeared, signifying complete loading of the salt.

The Interface 1010E potentiostat (Gamry instruments) and stainless-steel electrodes were used to carry out the impedance measurement. Samples were pressed into pellets (5 mm diameter) by applying a pressure of 3000 lbs. for 1 minute. The MOF maintains its structural integrity after being pressed as indicated from the powder X-ray diffraction (Figure S1). Pellets (thickness provided in tables S1 and S2) were then sandwiched between two 5 mm stainless steel electrodes and placed in a 2-electrode split test cell for R&D battery (EQ-STC, MTI Corporation). The impedance spectra were recorded by applying a range of frequencies from 1 MHz to 100 mHz with an amplitude of 10 mV. The sample cell was housed in an oven allowing the measurements to be conducted at 22, 40, 60, 70, 80, and 90 °C. Data analysis was conducted using the built-in Gamry software of the potentiostat and publication quality plots generated using OriginPro 2017. The ionic conductivity values were calculated using the impedance values from Nyquist plots with the measured cross-sectional area and thickness of the pellets (Table S1 and S2).

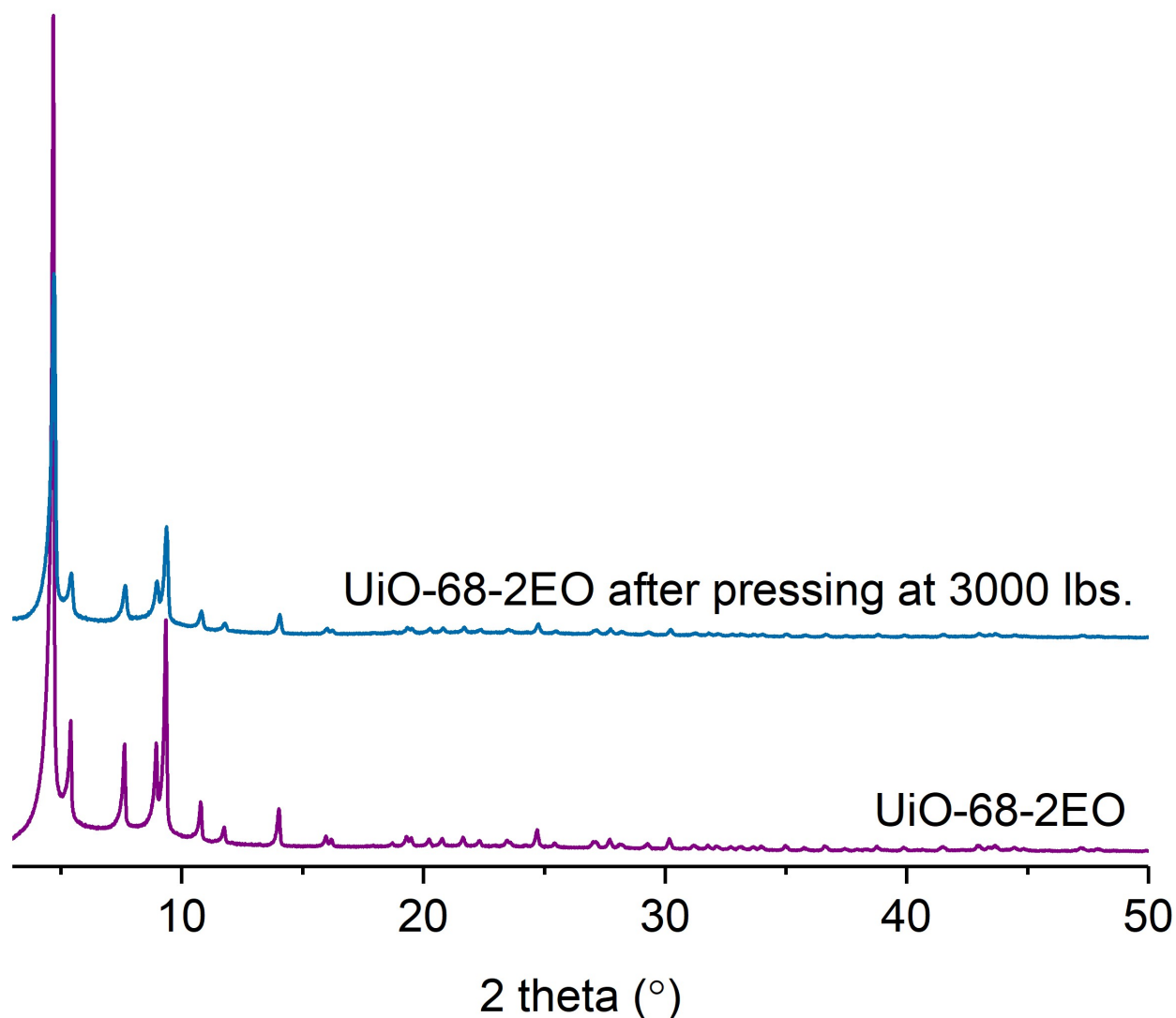


Figure S1. Comparison of powder X-ray diffraction patterns of UiO-68-2EO before and after application of 3000 lbs. pressure.

Calculated fractional void volume of each MOF and salt loading.

MOF	Fractional void volume	Max. theoretical LiTFSI loading (Mass %)	Max. experimental LiTFSI loading (Mass %)
UiO-68-EO	0.644	57.9	57.9
UiO-68-2EO	0.603	52.8	53.2

SI 2. NMR

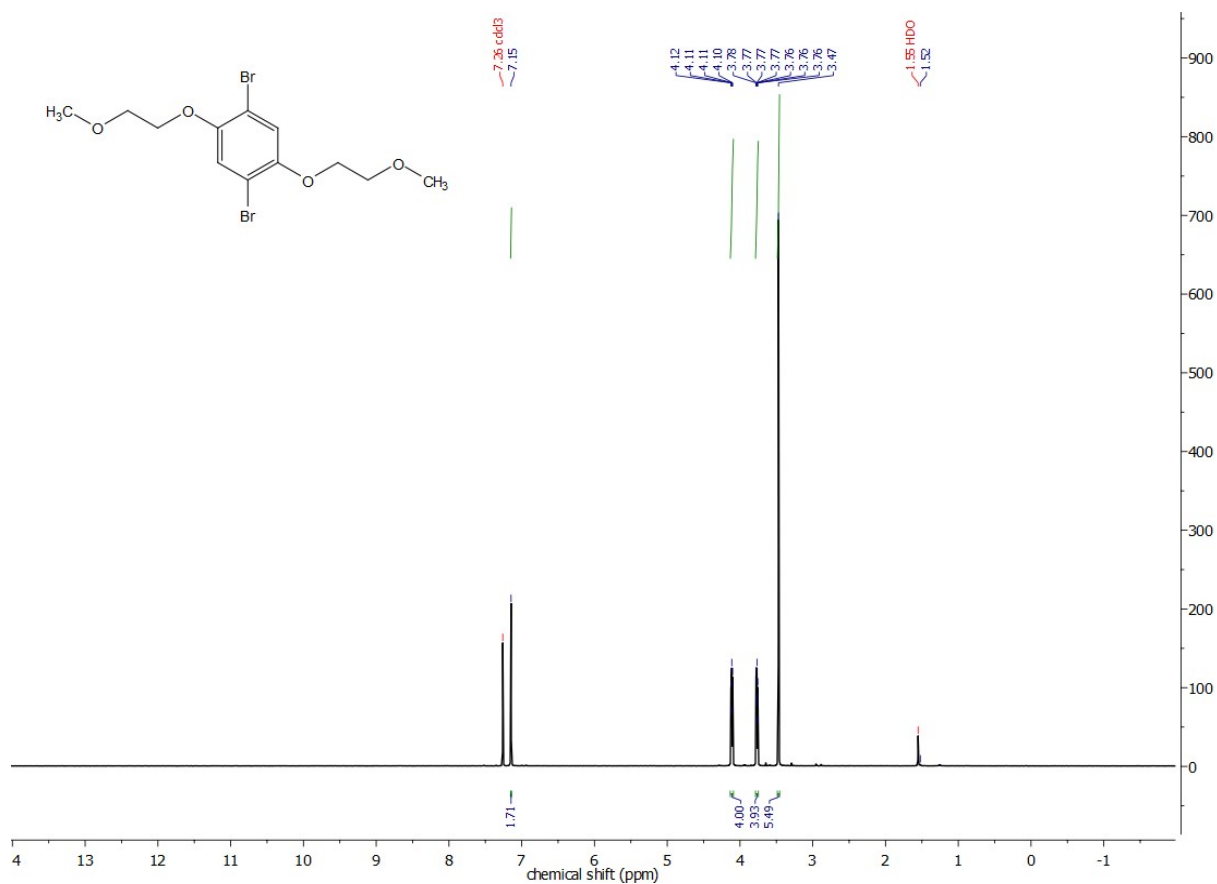


Figure S2. ¹H NMR (400 MHz) spectrum of 1,4-dibromo-2,5-bis(2-methoxyethoxy)benzene in CDCl₃

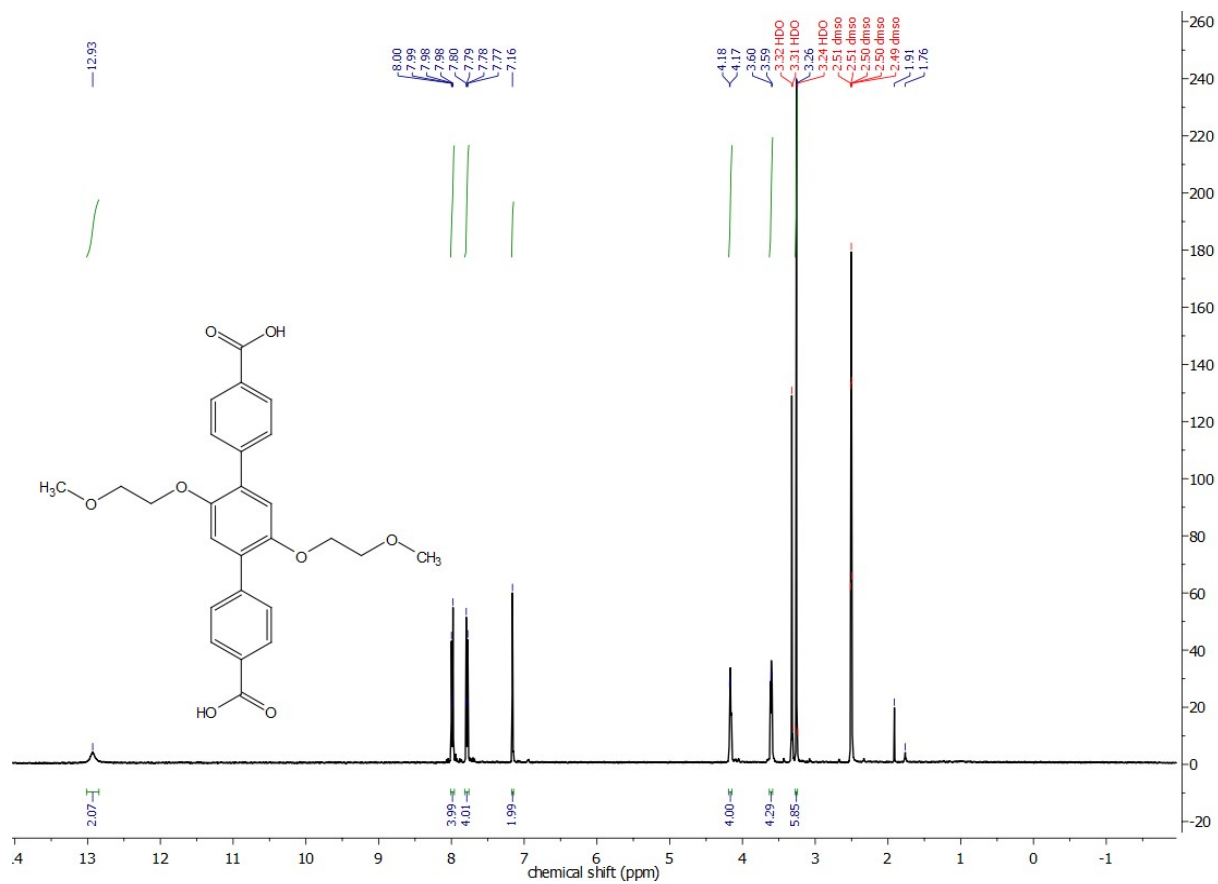


Figure S3. ^1H NMR (400 MHz) spectrum of 2',5'-bis(2-methoxyethoxy)-[1,1':4,1''-terphenyl]-4,4''-dicarboxylic acid in DMSO-d_6

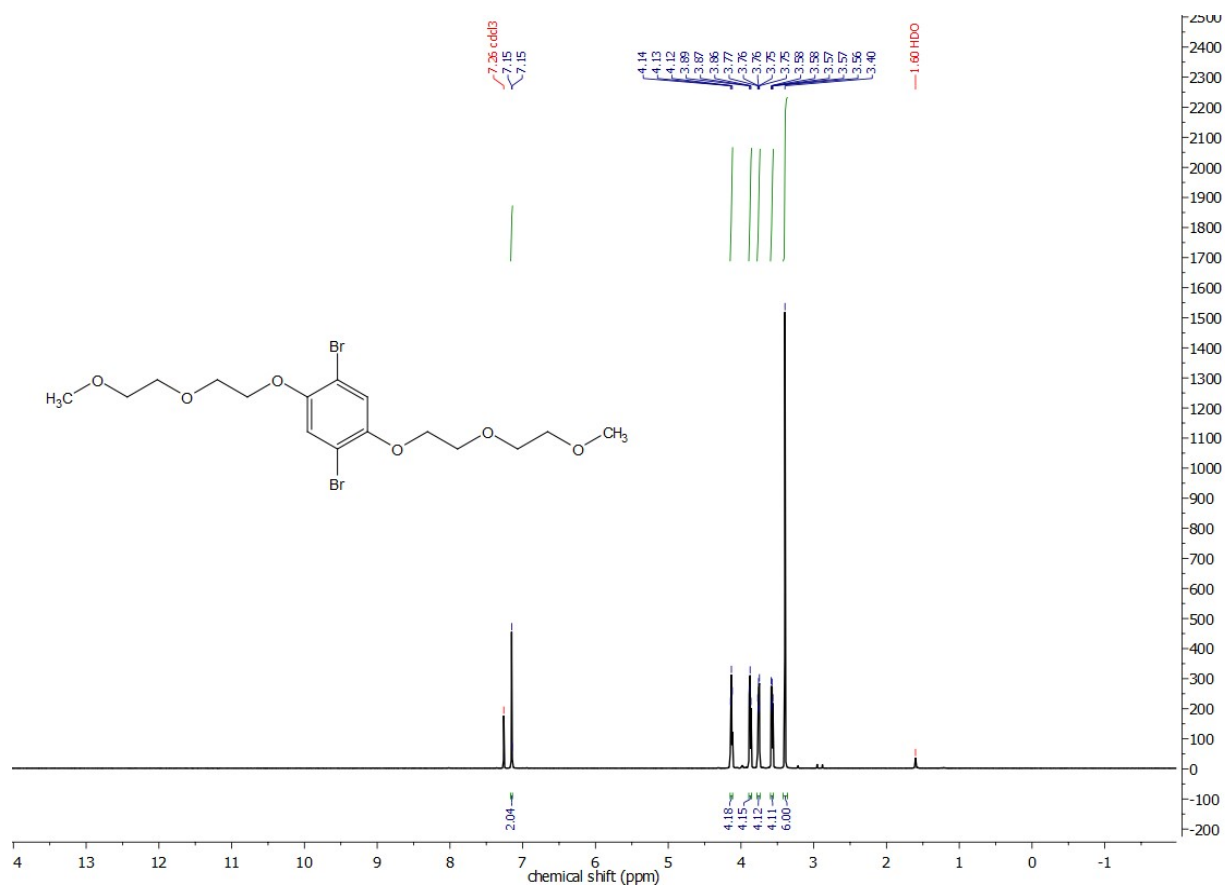


Figure S4. ¹H NMR (400 MHz) spectrum of (1,4-dibromo-2,5-bis(2-(2-methoxyethoxy)ethoxy)benzene) in CDCl₃

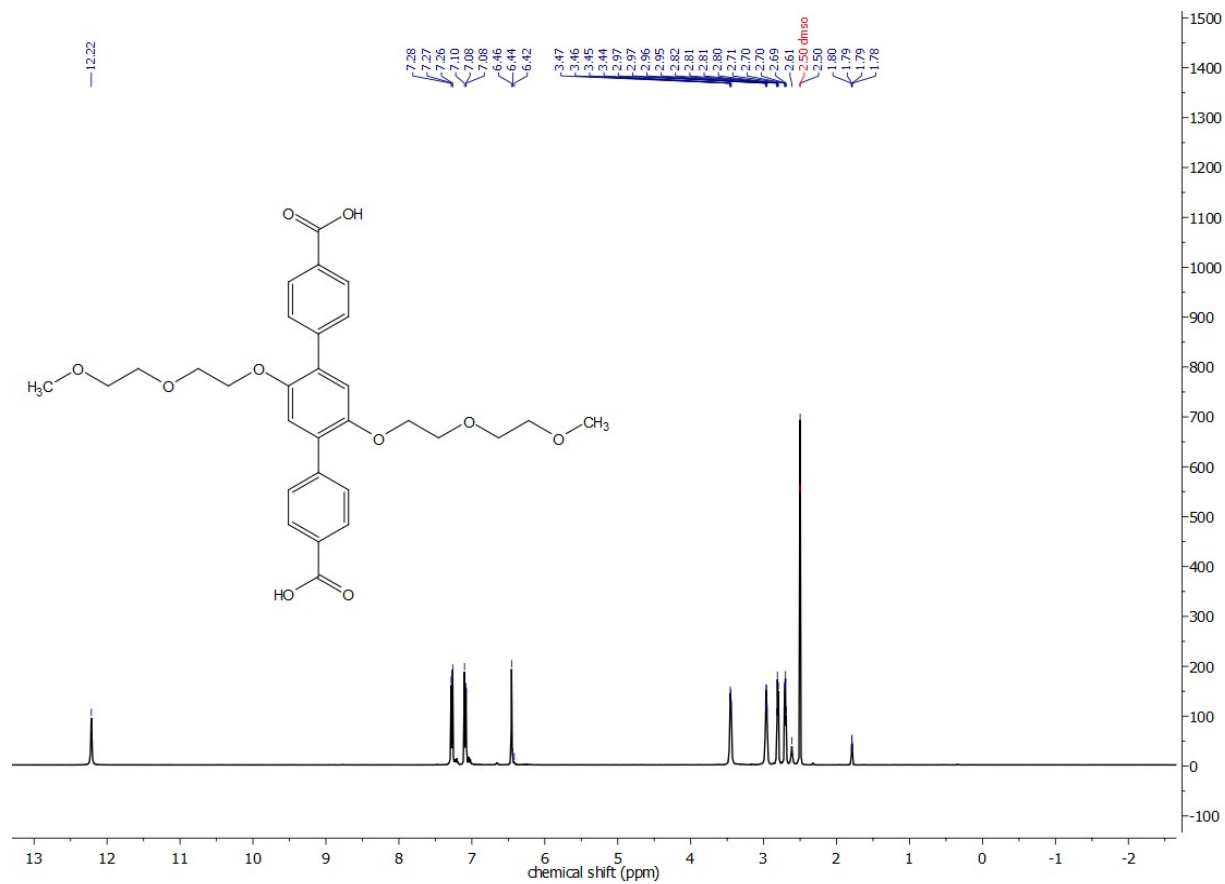


Figure S5. ^1H NMR (400 MHz) spectrum of 2',5'-bis(2-(2-methoxyethoxy)ethoxy)-[1,1':4',1''-terphenyl]-4,4''-dicarboxylic acid in DMSO-d_6

SI 3. Simulated and experimental PXRD patterns of MOFs

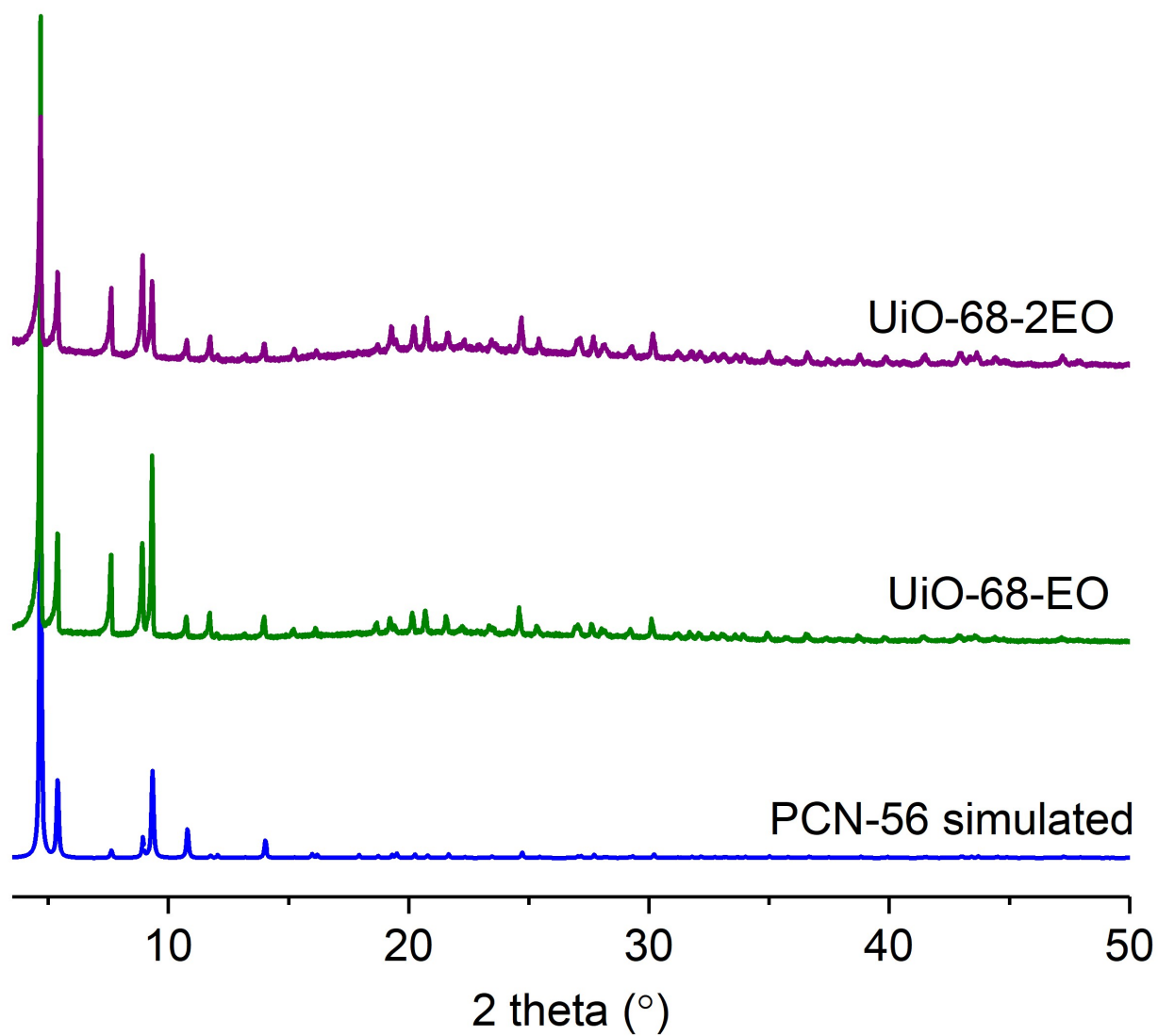


Figure S6. Comparison of experimental and simulated powder X-ray diffraction patterns of UiO-68-EO, UiO-68-2EO, and PCN-56 confirming their isostructurality.

SI 4. N₂ sorption isotherms for UiO-68-EO and UiO-68-2EO

N₂ sorption isotherms were measured on all MOFs prior to salt loading to ensure their phase purity and structural integrity.

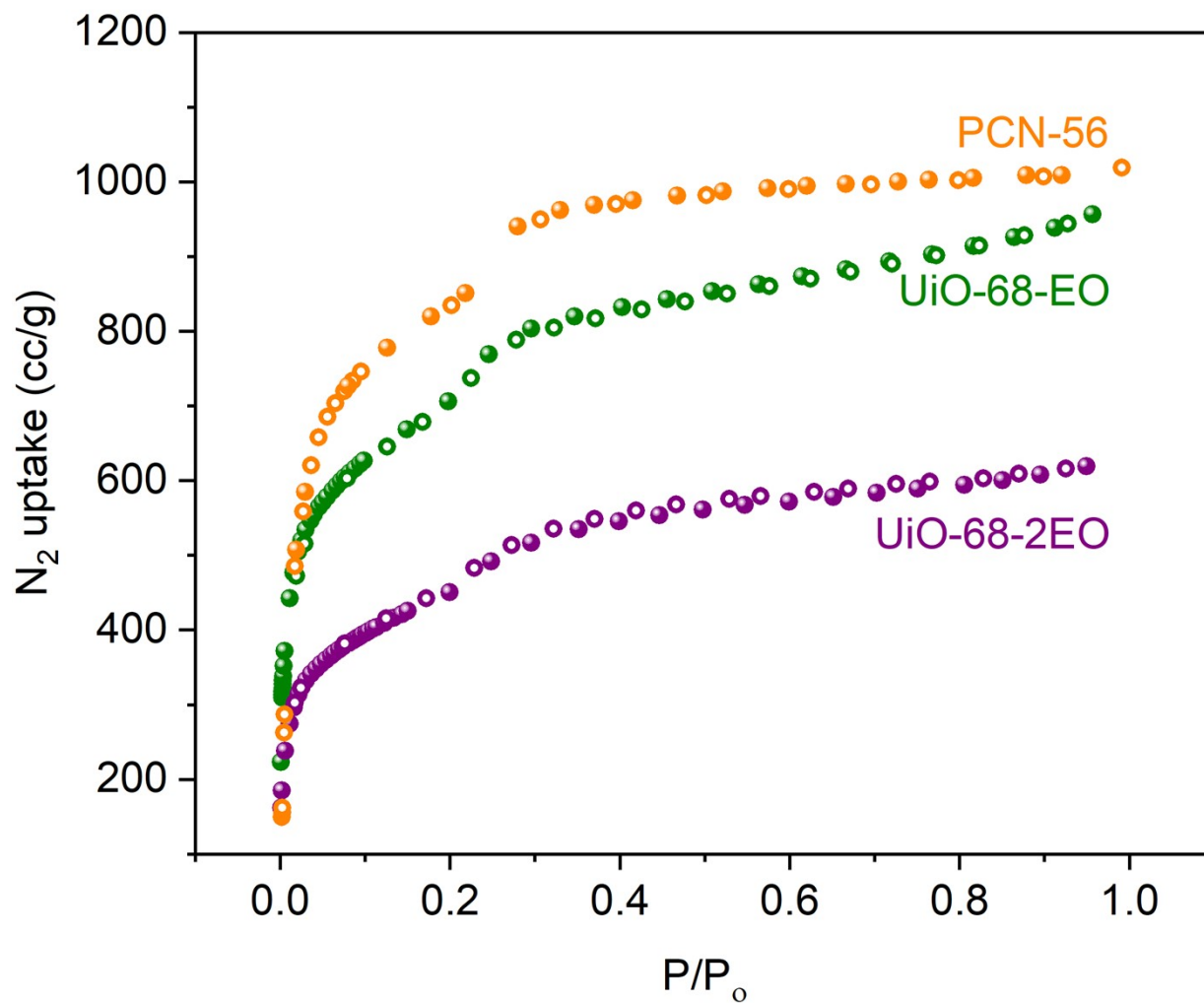
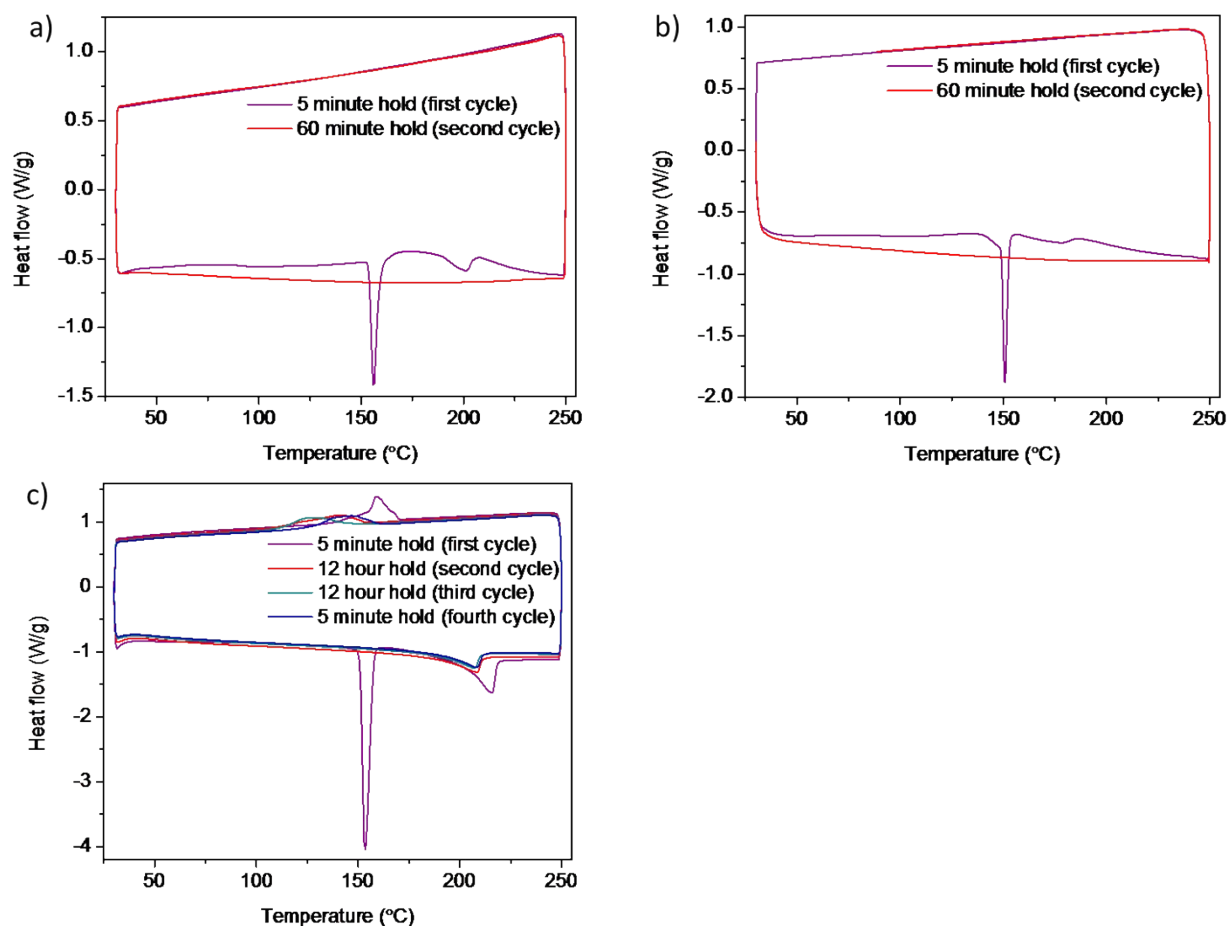


Figure S7. N₂ sorption isotherms of PCN-56, UiO-68-EO and UiO-68-2EO where the filled circles show adsorption and hollow circles show desorption at 77K.



SI 5. Cyclic DSC of UiO-68-2EO/LiTFSI composites

Figure S8. DSC traces of UiO-68-2EO/LiTFSI system; a) UiO-68-2EO 50 wt% LiTFSI, b) UiO-68-2EO 53.2 wt% LiTFSI, and c) UiO-68-2EO 55.7 wt% LiTFSI. The disappearance of the endotherm (LiTFSI melting) supports the complete loading of salt in 5 minutes for systems with 50 wt% and 53.2 wt% LiTFSI while the salt does not load completely even after 24 h for 55.7 wt% LiTFSI system suggesting the maximum loading of salt in UiO-68-2EO to be 53.2 wt%.

SI 6. PXRD of MOF-salt composites

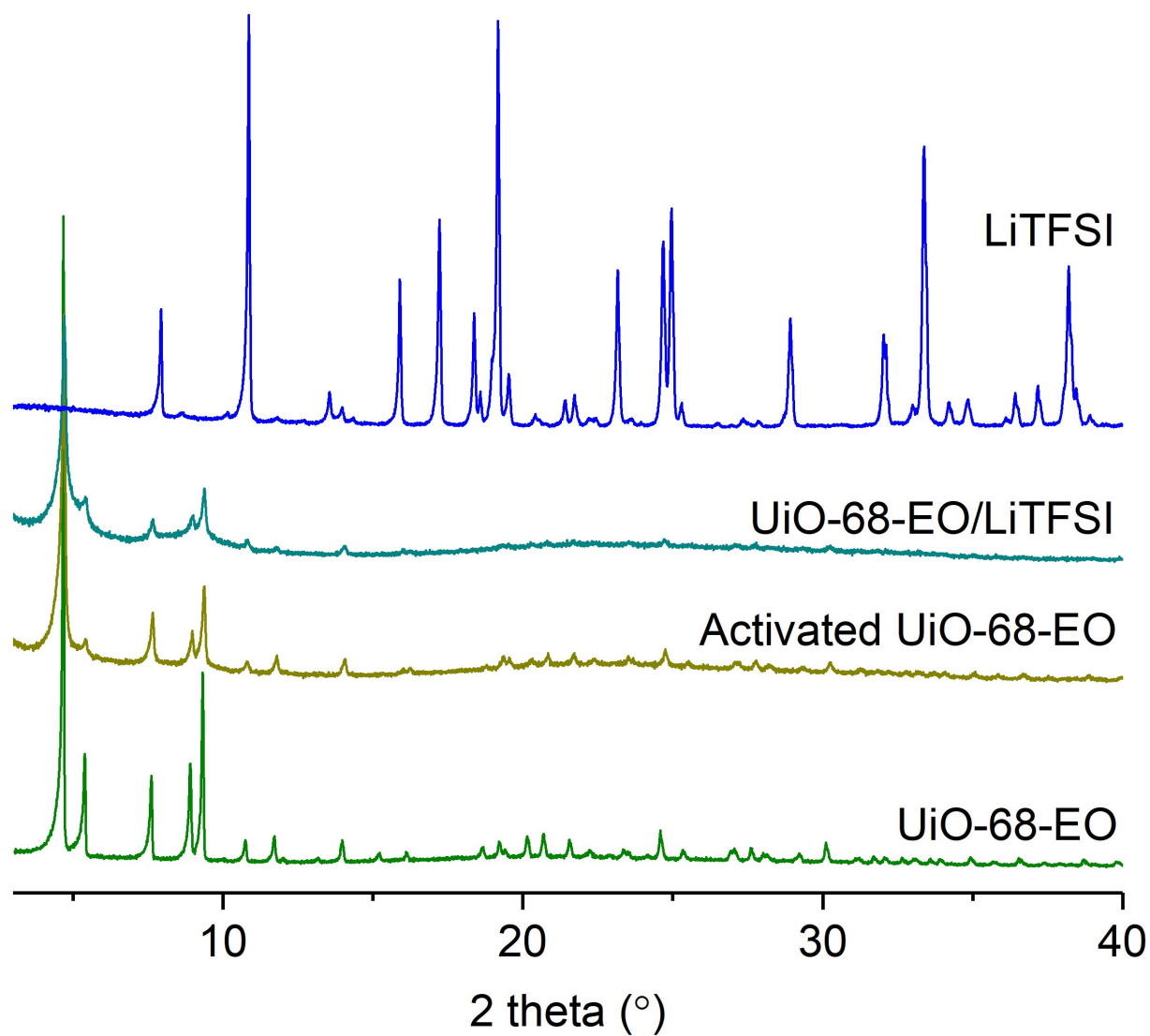


Figure S9. Comparison of powder diffraction patterns of UiO-68-EO (before and after activation), UiO-68-EO/LiTFSI composite and LiTFSI. Note the absence of LiTFSI diffraction peaks in the powder pattern of the composite.

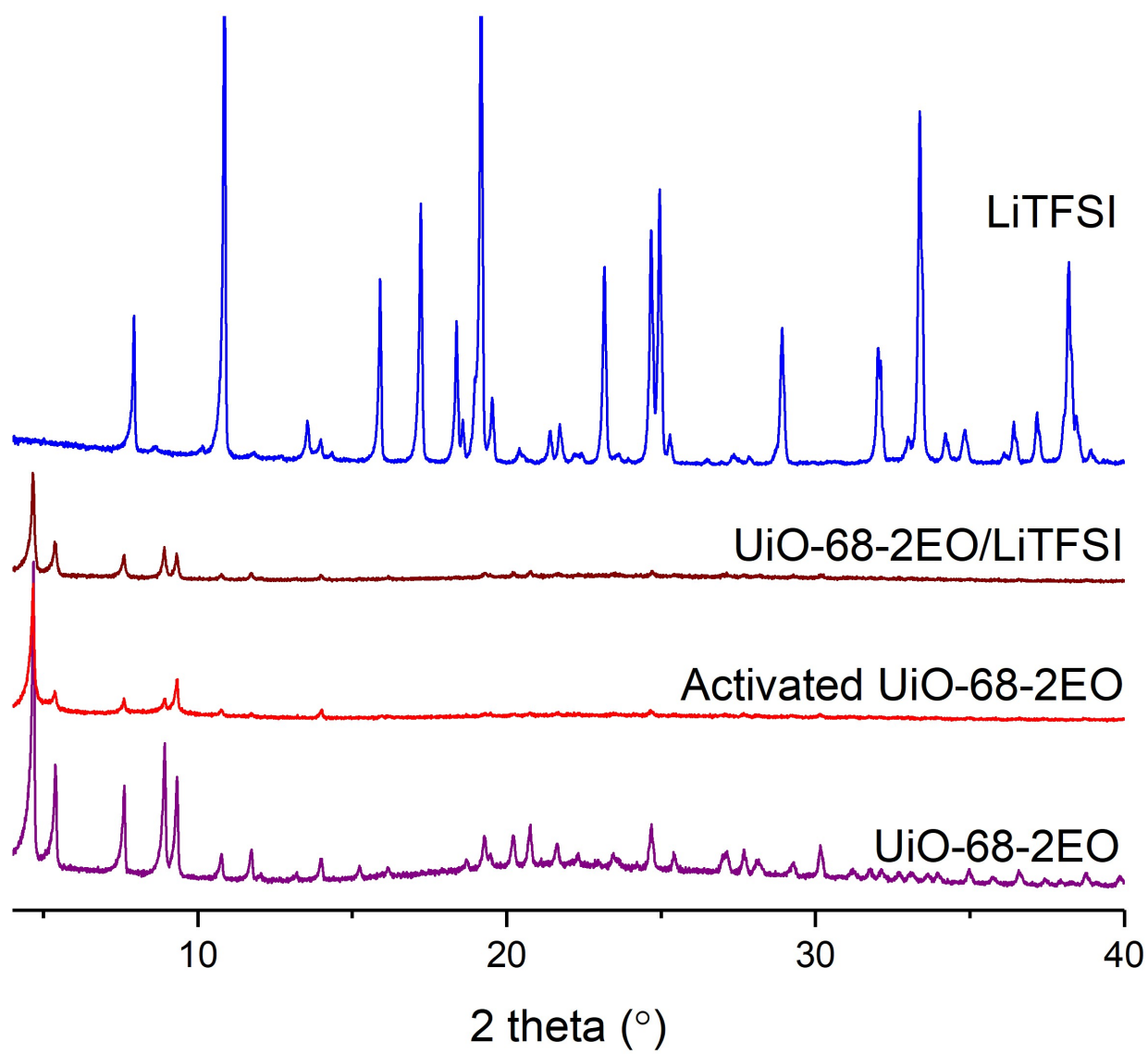


Figure S10. Comparison of powder diffraction patterns of UiO-68-2EO (before and after activation), UiO-68-2EO/LiTFSI composite and LiTFSI. Note the absence of LiTFSI diffraction peaks in the powder pattern of the composite.

SI 7. AC impedance spectroscopy

Temperature (°C)	Resistance (Ohms)	Thickness (cm)	Area (cm ²)	conductivity (S/cm)	1/T (K ⁻¹)	ln(Conductivity)	Activation Energy (eV)
22	131000000	0.065	0.193	2.57 x 10 ⁻⁹	0.003388	-19.7790108	0.76
40	17970000	0.065	0.193	1.87 x 10 ⁻⁸	0.003193	-17.79251718	
60	2837000	0.065	0.193	1.19 x 10 ⁻⁷	0.003002	-15.94656063	
70	1433000	0.065	0.193	2.35 x 10 ⁻⁷	0.002914	-15.26358363	
80	1090000	0.065	0.193	3.09 x 10 ⁻⁷	0.002832	-14.98999117	
90	885200	0.065	0.193	3.80 x 10 ⁻⁷	0.002754	-14.78187181	

Table S1. Calculation of ionic conductivity and activation energy of UiO-68-EO/LiTFSI

Temperature (°C)	Resistance (Ohms)	Thickness (cm)	Area (cm ²)	conductivity (S/cm)	1/T (K ⁻¹)	ln(Conductivity)	Activation Energy (eV)
40	1373356	0.079	0.193	2.98 x 10 ⁻⁷	0.003193	-15.02601027	1.3
60	64142.6	0.079	0.193	6.38 x 10 ⁻⁶	0.003002	-11.96210635	
70	20986.2	0.079	0.193	1.95 x 10 ⁻⁵	0.002914	-10.84486269	
80	4460	0.079	0.193	9.18 x 10 ⁻⁵	0.002832	-9.296146381	
90	1048	0.079	0.193	3.91 x 10 ⁻⁴	0.002754	-7.847881201	

Table S2. Calculation of ionic conductivity and activation energy of UiO-68-2EO/LiTFSI.

Table S3. Conductivity and activation energy comparison with existing MOFs and COFs

	Material	Conductivity (S/cm)	Act. Energy (eV)	Solvent and Temperature	Reference
1	COF-5-LiClO ₄	2.6 × 10 ⁻⁴	0.04	No solvent, RT	<i>J. Am. Chem. Soc.</i> 2016 , 138, 9767
2	TpPa-SO ₃ Li (LiOAc)	2.7 × 10 ⁻⁵	0.18	No solvent, RT	<i>J. Am. Chem. Soc.</i> 2019 , 141, 5880
3	Li-CON-TFSI	2.09 × 10 ⁻⁴	0.34	No solvent, 70 °C	<i>J. Am. Chem. Soc.</i> 2018 , 140(3), 896
4	TPB-BMTP-COF- LiClO ₄	5.49 × 10 ⁻⁴	0.87	No solvent, 90 °C	<i>J. Am. Chem. Soc.</i> 2018 , 140(24), 7429
5	UiO-68-2-EO/LiTFSI	3.9 x 10 ⁻⁴	1.3	No solvent, 90 °C	This study
6	COF-PEO-9-LiTFSI	1.2 x 10 ⁻⁴	N/A	No solvent, 100 °C	<i>J. Am. Chem. Soc.</i> 2019 , 141, 1227
7	Hyperbranched PEO-LiTFSI	1.3 x 10 ⁻⁴	N/A	No solvent, 100 °C	<i>Chem. Mater.</i> 2011 , 23, 2685
8	NUST-9-LiTFSI	2.6 x 10 ⁻³	0.32	1-butyl-1-methylpyrrolidinium bis-(trifluoromethanesulfonyl)i mide, 120 °C	<i>Chem. Mater.</i> 2021 , 33, 5058
9	CD-COF-Li ⁺ LiPF ₆ -EC-DMC	2.7 x 10 ⁻³	0.26	EC, DMC, RT	<i>Angew. Chem., Int. Ed.</i> 2017 , 56, 16313
10	H-Li-ImCOF	5.3 x 10 ⁻³	0.10	PC, RT	<i>J. Am. Chem. Soc.</i> 2019 , 141 (18), 7518
11	ICOF-2	3.05×10 ⁻⁵	0.24	PC, RT	<i>Angew. Chem., Int. Ed.</i> 2016 , 55, 1737
12	UiO-66-Li	1.1 × 10 ⁻⁴	0.21	No solvent, 90 °C	<i>ACS Appl. Energ. Mater.</i> , 2020 , 3, 4007
13	LPC@HKUST-1 (LiClO ₄)	3.8 x 10 ⁻⁴	0.62	PC, RT	<i>Adv. Mater.</i> 2018 , 30, 1707476

14	Mg-MOF-74-LiBF ₄ , LiOiPr	3.1×10^{-4}	0.15	EC, DEC, RT	<i>J. Am. Chem. Soc.</i> 2011 , 133, 37, 14522–14525
15	MIT-20d-LiBF ₄	4.8×10^{-4}	0.16	PC, RT	<i>J. Am. Chem. Soc.</i> 2017 , 139(38), 13260
16	[EHU1(Sc,Li)]-LiBF ₄	4.2×10^{-4}	0.25	DMC, RT	<i>Chem. Mater.</i> 2016 , 28, 2519
17	Al-Td-MOF-1	5.7×10^{-5}	0.11	PC, RT	<i>Angew. Chem., Int. Ed.</i> 2018 , 57, 16683
18	UiO-66-LiOtBu	1.8×10^{-5}	0.18	PC, RT	<i>Chem. Eur. J.</i> 2013 , 19, 5533
19	ZIF-67@ZIF-8-LiPF ₆	4.98×10^{-3}	0.18	EC/DMC/EMC, 100 °C	<i>Chem. Commun.</i> , 2020 , 56, 14629
20	ZIF-8-QSSE-LiPF ₆	1.0×10^{-3}	0.46	EC,DMC,EMC, 70 °C	<i>ACS Appl. Mater. Interfaces</i> , 2019 , 11, 46671
21	MOF-688-Li	3.4×10^{-4}	N/A	PC, RT	<i>J. Am. Chem. Soc.</i> , 2019 , 141, 17522
22	MOF-LiI	1.1×10^{-4}	0.24	PC, RT	<i>J. Am. Chem. Soc.</i> , 2019 , 141, 4422
23	UiO-67-LiTFSI	1.0×10^{-4}	N/A	1-Ethyl-3-methylimidazolium bis(trifluoromethanesulfonyl)imide, RT	<i>Nano Energy</i> , 2018 , 49, 580
24	UiO-66-LP-EMP	2.9×10^{-3}	0.07	EC, DEC, RT	<i>Adv. Mater.</i> , 2019 , 31, e1808338
25	Zr-BPDC-2SO ₃ H-LiTFSI	7.88×10^{-4}	0.16	PC, RT	<i>ACS Energy Lett.</i> 2021 , 6(7), 2434

SI 8. REFERENCES

1. Vazquez-Molina, D. A.; Pope, G. M.; Ezazi, A. A.; Mendoza-Cortes, J. L.; Harper, J. K.; Uribe-Romo, F. J. Framework vs. side-chain amphidynamic behaviour in oligo(ethylene oxide) functionalised covalent-organic frameworks. *Chem. Commun.*, **2018**, 54, 6947-6950.
2. Jiang, H.-L.; Feng, D.; Liu, T.-F.; Li, J.-R.; Zhou, H.-C. Pore surface engineering with controlled loadings of functional groups via click chemistry in highly stable metal-organic frameworks. *J. Am. Chem. Soc.* **2012**, 134 (36), 14690–14693.